Hindawi
Mobile Information Systems
Volume 2022, Article ID 2529041, 13 pages
https://doi.org/10.1155/2022/2529041

Research Article

Performance Analysis of Directional Ultra-Dense Networks with Dynamic Spectrum Partition Strategy

Qiaoshou Liu, Yingchen Gu, Jiaxin Wang, and Jianwen Zou

*School of Communication and Information Engineering,
Advanced Network and Intelligent Connection Technology Key Laboratory of Chongqing Education Commission of China,
Chongqing Key Laboratory of Ubiquitous Sensing and Networking, Chongqing University of Posts and Telecommunications,
Chongqing 400065, China*

Correspondence should be addressed to Yingchen Gu; 378180329@qq.com

Received 26 July 2022; Revised 18 December 2022; Accepted 19 December 2022; Published 31 December 2022

Academic Editor: Alessandro Bazzi

Intercell interference coordination (ICIC) plays a significant role in strengthening ultra-dense network (UDN) downlink coverage. From a statistical average perspective, a user is primarily interfered by its adjacent base station (BS), especially the second nearest BS. By modeling BSs equipped with directional antennas as a Poisson point process (PPP), this paper proposes a dynamic spectrum resource allocation strategy mainly about users' service BS and its nearest interference BS, where the subchannel assigned by the typical (served) user is interlaced from the channel simultaneously occupied by users within the effective radiation range of its second nearest BS. To fully explore this scheme for directional networks, we develop analytical expressions in terms of success probability and ergodic rate for the typical user based on the techniques of stochastic geometry, taking into account the fading of directional BS radiation angle. Then, we derive the meta distribution of the signal-to-interference ratio (SIR) for capturing individual link performance changes of users. Simulations verify the correctness of numerical results, and it is revealed that this strategy is in favor of users alleviating interference from their second nearest BSs and the performance advantages of the proposed ICIC strategy are better than those of the traditional directional UDNs.

1. Introduction

In accordance with the Ericsson Mobility Report, a quantity of subscribers will arrive at 7500 million and total global mobile data traffic will grow approximately 4.5 times to 226 EB per month by 2026 [1]. Ultra-dense networks (UDNs) are considered as a breakthrough to meet the traffic demand of 5G cellular networks [2]. By densely deploying small base stations (BSs) in the macro-cell to shorten the serving distance for users, the technology can reduce the coverage area of the macro-cell, thereby extending the network coverage area and increasing the system capacity [3, 4]. However, there exists a non-linear growth for the network capacity with the density of BSs [5]. In fact, such a promising deployment will negatively generate performance deterioration and severe network interference. LTE-A cellular downlink generally adopts frequency division multiple access or orthogonal frequency division multiple access (OFDMA) technology for diminishing or excluding the intracell cochannel interference [6]. It is a current challenge in wireless network research that different cells inevitably lead to mutual interference when they transmit on the same time-frequency resource block, i.e., intercell interference (ICI) [7]. Therefore, exploring and investigating interference management mechanics is essential to resist the adverse effect of grievous ICI in UDNs.

1.1. Motivation and Related Work. The directional antenna is introduced by jointly considering the development of the network, operation, and cost, which can greatly expand the coverage of wireless network [8]. In UDNs with directional antennas, signals can only be centralized transmission in a certain angular range unlike conventional isotropic antennas. A user receives ICI depending on whether the beams of neighboring cells collide with the beams of the cell where the user is located and the user is located in the beam crossing area. As a consequence, directional UDNs can effectively decrease the density of interference BSs while increasing the signal strength received by users. In [9–11], the authors proposed a three-dimensional directional network model to improve link reliability and system throughput by controlling ICI. A novel angle attenuation model was designed to simulate the angle declination of interference links in directional UDNs [12]. A virtual antenna array model and window function filtered weighting method based on directional antennas were proposed [13].

In recent years, there has been an explosion of studies on interference management in cellular networks. An available framework to analyze coverage probability and average rate of OFDM cellular network based on fractional frequency reuse (FFR) was explored [14]. In [15], the authors investigated various methods of ICIC and proposed new parameterized methods to classify them as dynamic and static ICIC strategies. The static ICIC schemes use methods to allocate subchannels (frequency bands) among cells and sectors, whereas dynamic schemes perform real-time cell coordination to allocate resources (frequency bands) to cells and sectors. In [16], a distributed self-learning ICIC scheme was proposed for autonomous networks under a model-free multi-agent reinforcement learning framework. The effect of FFR ICIC strategy on dynamic time-division duplex (D-TDD) network throughput was analyzed [17]. In [18], a novel soft frequency reuse together with decoupled association (DA) strategy was introduced to a heterogeneous cellular network (HetNet), which reduced ICI and improved network coverage. Furthermore, the authors of [19] presented a combination of Stienen's model and SFR HetNet deployment scheme to mitigate the ICI from MBS and improved the network performance gain. The authors of [20] proposed two ICIC strategies in millimeter-wave (mm-wave) cellular networks: one was only considering path loss including the blockage effect and another was based on both path loss and directivity gain.

To better assess the gains of directional UDNs with ICIC, a comprehensive network performance analysis is needed. Stochastic geometry is devoted to modeling and analyzing wireless cellular networks, which has extensively become a popular mathematical tool [21]. Coverage probability and ergodic rate, as two fundamental performance metrics, are derived by the spatial average of some point processes, especially by the Poisson point process (PPP). The coverage probability primarily refers to the proportion of users that can access the network for a certain SIR threshold. But it is not enough to give a precise reflection on the performance of edge users. To evaluate the authenticity of the independent links, further study of the meta distribution of the signal-to-noise ratio is required [22]. The meta distribution concentrates more detailed information on the proportion of successful probability for mobile users accessing the network. In [23], the authors evaluated outage probability and rate coverage of the user-centric two-tier network by Thomas cluster process modeling. In [24], the authors provided explicit expressions of the coverage probability in cellular networks modeled by PPP, which applied ICIC and intracell diversity (ICD). A distance-based ICIC for edge users in small cell networks was introduced in [25], and then the coverage probability of edge users was derived using stochastic geometry. The authors of [26] studied the coverage probability and average rate of downlink non-orthogonal multiple access for cellular-connected UAVs with user association ICIC scheme. However, the interference management strategies of cellular networks mentioned in the literature above are all from the level of network framework, without considering how to avoid intercell interference from the perspective of users. Their algorithms are highly complex and difficult to implement. On the other hand, none of these stochastic geometry-based models capture the fine-grained information about individual user distribution.

1.2. Contributions. The main contributions of this work can be summarized as follows:

(1) Tractable ICIC strategy for UDNs based on directional antennas: we develop a dynamic subchannel allocation strategy to study the performance of the UDNs with beamforming directional transmission. In particular, we consider a one-tier UDN, where BSs equipped with directional antennas are distributed as PPP. According to the ICI received by users mainly from the second nearby BSs, our spectrum resource strategy focuses on users' serving BS and their nearest interference BSs. To reduce or even eliminate the interference brought by the second nearest BS to a certain extent, when colliding with the beam of other cells, the channel partitioned by a user requesting communication is staggered with the channel occupied by users within the effective radiation range of the nearest interference BS at the same time.

(2) Coverage probability and transmission rate analysis: using stochastic geometry, we derive analytical expressions of coverage probability and ergodic rate under the proposed ICIC strategy. Also, the beam angle of the antenna is taken into consideration. Furthermore, the meta distribution of SIR is developed. In addition, some performance indexes like the variance of success probability and local delay can be obtained to assess the individual link information.

The rest of the paper is organized as follows. Section 2 introduces the system model considered in this paper. In Section 3, we present our spectrum resource allocation algorithm in relation to serving BS and closest interfering BS for the typical user. In Section 4, the theoretical expressions of performance indicators, i.e., coverage probability, ergodic rate, and the meta distribution of SIR, are derived. The numerical results and discussion are presented in Section 5. Finally, conclusions and extensions of future work are given in Section 6.

2. System Model

2.1. Downlink System Model. Consider a one-tier downlink UDN in which all users and BSs form two independent homogeneous Poisson point processes (HPPPs) Φ_u and Φ_s with densities λ_u and λ_s, respectively. The transmission power P_s of each BS is normalized to 1. All BSs directionally transmit messages to users by beamforming with directional antenna, whereas all users are equipped with isotropic antennas. The specific process of beamforming is beyond the scope of this article. The effective radiation angle of directional antenna is denoted as Ψ, $\Psi \in (0, 2\pi]$. Only users located in the range of Ψ can receive the expected or interference signals or else the communications link fails. The beam boresight direction φ_i of antennas is the central angle direction of the area it covers for each BS, which is an independent random variable on $(0, 2\pi]$. According to the Slivnyak theorem, we consider a virtual user $u_o \in \{u_t\}$ located at origin o as the typical user [27]. The i-th BS closest to u_o in Euclidean distance is denoted by $\{s_i\}$, where s_1 is the closest BS to u_o and the set of interference BSs for u_o is $\{\Phi_s \backslash s_1\}$. Without loss of generality, we let $\{R_i\}$ represent the distance between s_i and u_o from near to far, which can be denoted as $R_1 \leq R_2 \leq \ldots < R_i \leq \ldots$. For any users, in order to receive the strongest signal, Ψ of each BS adaptively and perfectly regulates the aiming direction of the beamforming to its serving user based on the position of its associated user in real time. In Figure 1, the signal link of user u_o used by red solid line represents the adaptive boresight directions φ_1 of its nearest BS s_1. To take full advantage of spectrum resources, all spectrum resources BW are reused by all BSs. Moreover, the OFDMA technology is employed in the proposed network to eliminate intracell interference.

The number of mobile users has increased rapidly; for this reason we consider the full load of the network so that all BSs' maintenance activity and all subcarriers are partitioned to their service users. A user communicates at most with one channel of its target BS, and a channel serves at most one user at the same moment. Considering that users choose BSs' access to the strongest received signal intensity, from the perspective of statistical average, the signal strength of BS received by the user increases as the distance from BS to the user decreases. In other words, the user chooses the nearest SBS as the service BS, which means that users will be subordinate to ICI from BSs other than their serving BSs.

We model the signal propagation considering path loss fading and small-scale fading (Rayleigh fading), where Rayleigh fading follows an independent and identically distributed (i.i.d) exponential distribution with unity, i.e., $h \sim \exp(1)$, and the path loss fading function is $\ell(R_i) = R_i^{-\alpha}, \alpha > 2$ [28]. The received power at the typical user u_o from s_1 is $hR_1^{-\alpha}$. For writing convenience, the subscript 1 of R_1 is omitted. Besides, this paper also considers the angle fading model of interference signal in [12]. The angular fading follows an exponential distribution, which only depends on the angle offset between the user position and the beam aiming directions of its interference BSs, i.e., $\xi(\theta_i) = e^{-|\theta_i|}$, where θ_i is an i.i.d random variable that represents the value of the angle offset between the location of u_o and the antenna boresight directions of its interfering BS. θ follows uniform distribution over 0 to 2π. When $\theta_i \notin [-(\Psi/2), \Psi/2]$, the value of function $\xi(\theta_i)$ is 0. In our proposed model, u_o will not be interfered by other BSs (except s_o) if it locates outside the effective radiation range of these BSs; otherwise, it will receive the interference signal from them.

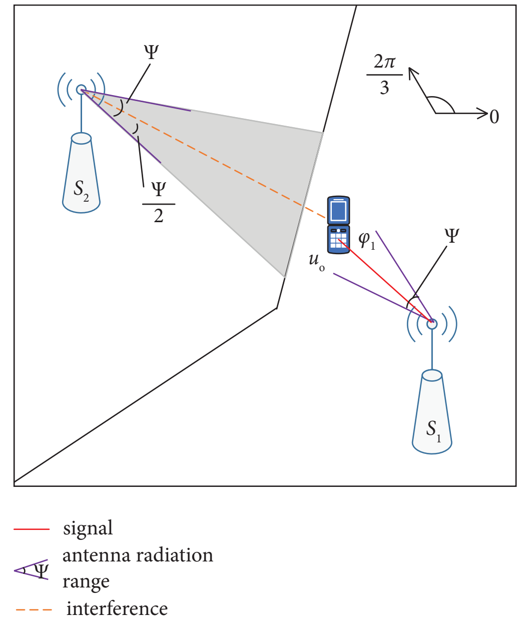

Figure 1: A dynamic subchannel allocation model for 2-D one-layer UDN, where Ψ is the directional radiation angle of each BS. The signal link (the red solid line) of u_o is the adaptive boresight direction φ_1 of its serving BS.

2.2. Analysis of User-Received Signal Strength. Let the random variable Z_i represent the strength of the signal received by the user from its i-th nearest BS, and the expectation is

$$\begin{aligned}\mathbb{E}[Z_i] &= \mathbb{E}[hR_i^{-\alpha}] \\ &= \mathbb{E}[h]\mathbb{E}[R_i^{-\alpha}] \\ &= \int_0^\infty r^{-\alpha} f_{R_i}(r)\mathrm{d}r,\end{aligned} \quad (1)$$

where $f_{R_i}(r)$ is the probability density function (PDF) of distance from u_o to its i-th nearest BS s_i. According to [29], it is given by

$$f_{R_i}(r) = \frac{(\lambda_s \pi r^2)^{i-1}}{(i-1)!} 2\pi\lambda_s r e^{-\lambda_s \pi r^2}. \quad (2)$$

When $i - \alpha/2 > 0$, (2) can be simplified as

$$\mathbb{E}[Z_i] = \frac{(\lambda_s\pi)^{\alpha/2}}{(i-1)!}\Gamma\left(i - \frac{\alpha}{2}\right), \tag{3}$$

where the function $\Gamma(n) = \int_{x>0} x^{n-1}e^{-x}\mathrm{d}x, n > 0$ is the standard gamma function. Let $N_0 = \lceil i - \alpha/2 \rceil$, where the function $\lceil \cdot \rceil$ is is rounded up. Then, the expectation of u_o receiving the accumulative sum of signal intensity from the N_0-th to the N_s-th BS is

$$\sum_{i=N_0}^{N_s} \mathbb{E}[Z_i] = (\lambda_s\pi)^{\alpha/2}\left(\frac{1}{N_0 - 2} - \frac{1}{N_s - 1}\right), \tag{4}$$

where N_s is the number of all BSs around the whole network. Considering the outdoor situation and the special value $\alpha = 4$, we derive $N_0 = 3$. So, equation (4) can be further simplified as

$$\sum_{i=3}^{N_s} \mathbb{E}[Z_i] = (\lambda_s\pi)^2\left(\frac{N_s - 1}{N_s - 2}\right) \approx (\lambda_s\pi)^2, \tag{5}$$

where the case of $i = 1, 2$ needs to be obtained according to equation (1). It can be deduced from equations (4) and (5) that the signal intensity of the second nearest BS received by a user is lower than the sum of the signal intensity of all interfering BSs (including the second nearest BS). From the statistical perspective of spatial average, if the user chooses the nearest BS as the target BS, the effective signal received by the user is the strongest. The interference received by users mainly comes from the second BS, and it predominates in the interference signal. The discussion of the ICIC strategy that effectively mitigates the second nearest BS to the user's interference will be given in the next section.

3. Dynamic Subchannel Allocation Strategy Based on Directional Antenna

From the perspective of spatial statistical average, the user's association with the nearest SBS means that the user's interference mainly comes from its second nearest SBS. If the interference caused by the second nearest SBS can be weakened or eliminated, the SIR value of the signal received by users can be significantly improved and the communication experience of users can be improved. In order to achieve this goal, the subchannel allocation ICIC (SA-ICIC) scheme is determined by jointly considering the typical user's nearest and second nearest BS.

As shown in Figure 1, we assume s_2 is the nearest interference BS for u_o. When the typical user u_o accesses the nearest BS s_o, s_o randomly allocates any idle subchannel among all channels to u_o. Without loss of generality, it is assumed that s_o randomly selects subchannels B_j to be assigned to u_o; the discussion of whether the subchannel B_j can be used is as follows:

(1) If the subchannel B_j is not occupied by any user in the cell covered by s_2, s_o can assign B_j to u_o and tell s_2 that B_j cannot be allocated to the users located within the radiation range of s_2 at the same time, namely, users radiated by the shaded part in Figure 1.

(2) If $B_j$is used by a user in the non-shaded part of the cell covered by s_2, i.e., all users in the shaded part of the cell covered by s_2 are not occupied the B_j, in this case, $s_o$can assign the subchannel B_j to $u_o$and inform s_2 cannot be allocated B_j to users radiated by the shaded part of cell s_2.

(3) If B_j is used by a user in the shaded part of the cell covered by s_2, s_o should select other idle subchannels to allocate to u_o, but it needs to avoid the subchannels used by users in the shaded part of the cell covered by s_2.

(4) In case of non-free subchannels for s_o, B_j can only be allocated to u_o by s_o.

In the dynamic SA-ICIC based on directional antenna shown in Figure 1, it only needs to consider the service SBS and the second nearest BS of any user requesting communication. The specific subchannel allocation scheme is shown in Algorithm 1, where N_s is the number of all BSs in the UDNs, N_c is the number of available subchannels of each BS, $N_{i,u}$ is the number of users served by i-th BS, $\theta_{se,t}$ is the angular offset of the t-th user and its second nearest SBS beam boresight direction, $C_{se,j}$ is the available range of j-th subchannel of the second BS for t-th user, and $C_{sh,t}$ is the coverage area centered on the line between u_o and its second nearest BS with each of the left and right angles $\Psi/2$ (the shaded part in Figure 1). $N_{i,j}$indicates whether the j-th subchannel of the i-th BS is occupied, to be specific, $N_{i,j} = 0$ represents the channel is not occupied, $N_{i,j} = 1$ instead.

We consider that the network is interference-limited because the influence of thermal noise on UDN is negligible compared with interference. The cumulative interference function of u_o is

$$I_{s,s} = G \cdot \sum_{i=2} A_i, \tag{6}$$

where $A_i = h_i\xi(\theta_i)R_i^{-\alpha}, i \in \{2, 3, \ldots, N_s\}$, $G = (1 + (\Psi/2\pi) \cdot ((\Psi/2\pi) - 1))$. There are N_s terms totally added in parentheses according to Newton's binomial theorem.

Proof. Assuming that the subchannel B_j is allocated to u_o, we let $A_i = h_i\xi(\theta_i)R_i^{-\alpha}, i \in \{2, 3, \ldots, N_s\}$. Let η represent the interference probability of any SBS to u_o, so η is equal to $\Psi/2\pi$. Then, the signal strength received by u_o from all SBSs is arranged and summed by binary counting method ("0" represents that BSs interfere with u_o, i.e., there is a coefficient η, while "1" represents that BSs do not interfere with the user, i.e., there is no η). The sum of the cumulative interference received by the typical user u_o is given by

$$I_d = \left(\eta A_1 + \eta A_2 + \cdots + \eta A_{N_s-1} + \eta A_{N_s}\right) \cdot p_t^{N_s} + \left(\eta A_1 + \eta A_2 + \cdots + \eta A_{N_s-1} + A_{N_s}\right) \cdot p_t^{N_s-1} p_{\bar{t}} + \left(A_1 + A_2 + \cdots + A_{N_s-1} + \eta A_{N_s}\right) \cdot p_t p_{\bar{t}}^{N_s-1} + \left(A_1 + A_2 + \cdots + A_{N_s-1} + A_{N_s}\right) \cdot p_{\bar{t}}^{N_s}, \quad (7)$$

where $p_t = \Psi/2\pi$ represents the probability that u_o receives interference and $p_{\bar{t}} = 1 - \Psi/2\pi$ is the probability that u_o does not receive interference. According to the Newton's binomial theorem, there are N_s terms in the parentheses on the right of the equal sign to add.

Summing the right side of equation (7) by column, the expression of the sum of each column is

$$I_i = p_t \sum_{s_i \in \Phi_a \backslash \{s_o\}} C_{N_s-1}^k p_t^k p_{\bar{t}}^{N_s-1-k} \cdot \eta A_i + p_{\bar{t}} \sum_{s_i \in \Phi_a \backslash \{s_o\}} C_{N_s-1}^k p_t^k p_{\bar{t}}^{N_s-1-k} \cdot A_i \overset{(a)}{=} p_t \left(p_t + p_{\bar{t}}\right)^{N_s-1} \eta A_i + p_{\bar{t}} \left(p_t + p_{\bar{t}}\right)^{N_s-1} A_i = \left(1 + \frac{\Psi}{2\pi} \cdot \left(\frac{\Psi}{2\pi} - 1\right)\right) A_i, \quad (8)$$

where step (a) follows the binomial theorem. By summing all columns of equation (7), we can obtain the expression of interference received by u_o:

$$I_{s,s} = \left(1 + \frac{\Psi}{2\pi} \cdot \left(\frac{\Psi}{2\pi} - 1\right)\right) \cdot \sum_{s_i \in \{\Phi_s \backslash s_o\}} A_i = \left(1 + \frac{\Psi}{2\pi} \cdot \left(\frac{\Psi}{2\pi} - 1\right)\right) \cdot \sum_{s_i \in \{\Phi_s \backslash s_o\}} h_i \xi(\theta_i) R_i^{-\alpha}. \quad (9)$$

So, the SIR received by the user is

$$\mathrm{SIR} = \frac{hR^{-\alpha}}{G \cdot \sum_{i=2} A_i}, \quad (10)$$

where $A_i = h_i l(\theta_i) R_i^{-\alpha}, i \in \{2, 3, \ldots, N_s\}$, $G = (1 + (\Psi/2\pi) \cdot ((\Psi/2\pi) - 1))$. □

4. Analytical Model

In this section, we derive analytical expressions to evaluate our proposed network with the SA-ICIC scheme. First, the expressions of the coverage probability and ergodic rate of networks are derived. Then, a much sharper version provided by meta distribution of the SIR is obtained. Furthermore, some fine-grained information like the variance of conditional success probability and the mean local delay can be acquired.

4.1. Coverage Probability. The coverage probability can be regulated as the probability that SIR of a typical user exceeds a given threshold for successfully demodulating and decoding. Mathematically, it can be expressed as $p_c(T, \lambda_s, \alpha, \Psi) \triangleq \mathbb{P}[\mathrm{SIR} > \beta], \beta \in \mathbb{R}$, where β is the target SIR threshold of cellular link. We now characterize the coverage probability using the SA-ICIC algorithm presented above.

Theorem 1. *In the proposed SA-ICIC strategy network model based on the directional antenna, the coverage probability of the network is as follows:*

$$p_c(T, \lambda_s, \alpha, \Psi) = \pi\lambda_s \int_0^\infty e^{-\left(\lambda_s \pi v + \left(2\lambda_s v TG/\alpha - 2\right) C_1(T,\alpha,\Psi)\right)} \mathrm{d}v, \quad (11)$$

where $C_1(T, \alpha, \Psi) = \int_0^{\Psi/2\pi} e_2^{-\theta} F_1[1, 1 - (2/\alpha), 2 - (2/\alpha), -(TG/e^{\theta})] \mathrm{d}\theta$ *and* ${}_2F1[\cdot,\cdot,\cdot,\cdot]$ *is the* Gaussian *hypergeometric function.*

Proof. The distance from u_o to its nearest BS s_1 is denoted as R; then, the success probability of accessing the network for u_o is expressed as

$$P[\mathrm{SIR} > T] = E_R[P[SIR > T|R]] = \int_0^\infty P\left[h > Tr^\alpha I_{s,s} \middle| r\right] f_R(r) \mathrm{d}r \overset{(a)}{=} \int_0^\infty \mathscr{L}_{I_{s,s}}(Tr^\alpha) f_R(r) \mathrm{d}r, \quad (12)$$

where the PDF of R is according to equation (2) ($f_R(r) = 2\pi\lambda_s r e^{-\lambda_s \pi r^2}$). Step (a) follows from Rayleigh distribution $h \sim \exp(1)$. $I_{s,s}$ is the cumulative interference received by u_o and its Laplace transform function $\mathscr{L}_{I_{s,s}}(Tr^\alpha)$ is equal to $\mathscr{L}_{I_{s,s}}(s) = E_{I_{s,s}}[e^{-sI_{s,s}}]$. Letting $s = Tr^\alpha$,

$$\begin{aligned}\mathscr{L}_{I_{s,s}}(Tr^{\alpha}) &= \mathscr{L}_{I_{s,s}}(s) = E_{I_{s,s}}\left[e^{-sI_{s,s}}\right]\\ &= E_{\Phi,h_i,\theta_i}\left[e^{-s(1+(\Psi/2\pi)\cdot((\Psi/2\pi)-1))\cdot\sum_{i=2}h_i\xi(\theta_i)R_i^{-\alpha}}\right]\\ &\overset{(a)}{=} E_{\Phi}\left[\prod_{i=2}E_{\theta}\left[\frac{1}{s((1+(\Psi/2\pi))\cdot((\Psi/2\pi)-1))\cdot R_i^{-\alpha}\left(1/e^{|\theta|}\right)+1}\right]\right],\end{aligned} \tag{13}$$

where step (a) is obtained by using the probability generating functional (PGFL) lemma. Let $G = (1 + (\Psi/2\pi)\cdot((\Psi/2\pi) - 1))$. Combined with the PDF of θ is $(\theta) = 1/2\pi$, equation (13) can be simplified as

$$\mathscr{L}_{I_{s,s}}(Tr^{\alpha}) = \exp\left(-2\lambda_s\int_r^{\infty}\left(\frac{1}{(sGv^{-\alpha})^{-1}e^{\theta}+1}\mathrm{d}\theta\right)v\ \mathrm{d}v\right). \tag{14}$$

Let $((sG)^{-1}e^{\theta}v^{\alpha})^{2/\alpha} = u$, $du = 2v((sG)^{-1}e^{\theta})^{2/\alpha}\mathrm{d}v$, and the Laplace transform of the cumulative interference function $I_{s,s}$ is

$$\mathscr{L}_{I_{s,s}}(Tr^{\alpha}) = \exp\left(-\frac{2\lambda_s r^2 T\times G}{\alpha-2}\times\int_0^{\Psi/2\pi} e_2^{-\theta}F_1\left[1,1-\frac{2}{\alpha},2-\frac{2}{\alpha},-Te^{-\theta}G\right]\mathrm{d}\theta\right). \tag{15}$$

Combining it with (12), (11) is obtained. □

Lemma 1. *In the SA-ICIC strategy network model based on directional antennas, if the interfering link does not experience angle fading, it can be approximated as $|\theta_i| = 0$ in equation (11). That is to say, it is a resemblance to the conventional omnidirectional antenna in that the link only experiences path loss and fast fading. Then, the probability of u_o accessing the network successfully is*

$$p_c(T,\lambda_s,\alpha,\Psi) = \pi\lambda_s\int_0^{\infty} e^{-\left(\lambda_s\pi v+\left(2\lambda_s vTG/\alpha-2\right)C_2(T,\alpha)\right)}\mathrm{d}v, \tag{16}$$

where $C_2(T,\alpha) = {}_2F_1[1,1-(2/\alpha),2-(2/\alpha),-(TG/e^{\theta})]$.

4.2. Ergodic Rate. The ergodic rate of users is $\mathbb{E}[\ln(1+\mathrm{SIR})]$. Exploiting the fact that $\ln(1+\mathrm{SIR})$ is a monotonically increasing function of SIR, we arrive at

$$\tau = \int_{t>0}\mathrm{P}\left[\mathrm{SIR}>2^t-1\right]\mathrm{d}t. \tag{17}$$

Thus, the average rate is equivalent to the coverage probability evaluated at $T = 2^t - 1$ and is then integrated with respect to t. The coverage of a typical user is given by equation (11); thus, the average rate of u_o can be obtained by substituting $T = 2^t - 1$ into equation (11), and integrating the result over t, the final expression is given by Theorem 2.

Theorem 2. *According to the proposed ICIC strategy, the average ergodic rate of u_o is computed as*

$$\tau(\alpha,\Psi) = \pi\lambda_s\times\int_0^{\infty}\int_0^{\infty}\exp\left(-2\lambda_s v\left(e^t-1\right)G\times C_3(\alpha,\Psi)-\lambda_s\pi v\right)\mathrm{d}v\mathrm{d}t, \tag{18}$$

where $C_3(\Psi,\alpha) = \int_0^{\Psi/2\pi} e_2^{-\theta}F_1[1,1-(2/\alpha),2-(2/\alpha),-(e^t-1)e^{-\theta}G]d\theta/(\alpha-2)$.

Lemma 2. *The absolute value of the angle offset variable is identical to Lemma 1 when neglecting the angle fading, which can be approximated as $|\theta_i| = 0$. The average ergodic rate of the typical user is then obtained as*

(1) Initialize: $N_{i,j} = 0$, $C_{se,j} = [0, 2\pi)$.
(2) **for** $i = 1$ to N_s **do**
(3) Calculate $N_{i,u}$;
(4) **for** $t = 1$ to $N_{i,u}$ **do**
(5) Calculate $\theta_{se,t}$ and then obtain the shaded area coverage $C_{sh,t}$;
(6) **for** $j = 1$ to N_c **do**
(7) **if** $j \neq N_c$ **then**
(8) **if** $N_{i,j} = 0$ **then**
(9) **if** $\varphi_{se,j} == \phi$ or $\varphi_{se,j} \in [0, 2\pi)/C_{sh,t}$ **then**
(10) Subchannel B_j is assigned to to u_t;
(11) Mark $C_{se,j} = C_{se,j}/C_{sh,t}$;
(12) Mark $N_{i,j} = 1$;
(13) break;
(14) **else if** $\varphi_{se,j} \in C_{sh,t}$ **then**
(15) Return to line 5;
(16) **end if**
(17) **else if** $N_{i,j} = 1$ **then**
(18) Return to line 5;
(19) **end if**
(20) **else**
(21) Select an idle subchannel B_j to assign it for u_t;
(22) Mark $C_{se,j} = C_{se,j}/C_{sh,t}$ *;
(23) Mark $N_{i,j} = 1$;
(24) **end if**
(25) **end for**
(26) **end for**
(27) **end for**
* If used, the tag is invalid.

Algorithm 1: Dynamic subchannel allocation strategy based on directional antenna.

$$\tau(\alpha, \Psi) = \pi\lambda_s \times \int_0^\infty \int_0^\infty \exp\left(-\Psi\lambda_s vG\left(e^t - 1\right)C_4(\alpha, \Psi) - \lambda_s \pi v\right) dv\, dt, \tag{19}$$

where $C_4(\Psi, \alpha) = {}_2F_1[1, 1 - (2/\alpha), 2 - (2/\alpha), -(e^t - 1)G]/\alpha - 2$.

4.3. The Meta Distribution of Directional Network. The complementary cumulative distribution function (CCDF) of the conditional SIR of the typical user given the points processes is

$$P_s(T) \triangleq \mathbb{P}(\mathrm{SIR}_o > T \mid \Phi), \tag{20}$$

which is the random variable. Meta distribution $\overline{F}_{P_s}(x)$ is the CCDF of the conditional success probability. Hence, the meta distribution is formally given by

$$\overline{F}_{P_s}(x) \triangleq \mathbb{P}^o\left(P_s(T) > x\right), x \in [0, 1], \tag{21}$$

where $\mathbb{P}^o$ is the Palm measure, provided that the typical receiver and its corresponding service source are active. As all point processes in the model are ergodic, the meta distribution can be translated as the fraction of the active links whose conditional success probabilities are greater than x.

The b-th moment of P_s is denoted by M_b, i.e., $M_b \triangleq \mathbb{E}^0(P_s^b)$. In this paper, the beta approximation method is used to formulate the meta distribution [30], which requires only the first and second moments. Accordingly, the b-th moment of $P_s(\beta)$ is given by

$$M_b(\beta) \triangleq \mathbb{E}\left[P_s(\beta)^b\right] = \int_0^1 bx^{b-1}\overline{F}_{P_s}(x)\mathrm{d}x, b \in \mathbb{Z}. \tag{22}$$

Some important performance characteristics are acquired through equation (22). They include $p_s(\beta) \equiv M_1(\beta)$, the variance $M_2 - M_1^2$ of $P_s(\beta)$, and the mean local delay M_{-1} from the −1-st moment of $P_c(\beta)$.

Theorem 3. *Under the proposed SA-ICIC strategy network model based on directional antennas, the b-th moment of the conditional success probability of u_o accessing the network is*

$$M_b = \pi\lambda_s \times \int_0^\infty \exp\left(-\lambda_s v C_5(T,\alpha,\Psi) - \lambda_s \pi v\right)\mathrm{d}r, \alpha > 2, b \in \mathbb{C}, \tag{23}$$

where $C_5(T,\alpha,\Psi) = \int_0^{\Psi/2} {}_2F_1[1, 1-(2/\alpha), 2-(2/\alpha), -Te^{-\theta}G] - 1\mathrm{d}\theta.$

Proof. In a given point process Φ_s, the conditional success probability of the typical user u_o is

$$\begin{aligned} P_c(T) &= \mathbb{P}(\mathrm{SIR} > T \mid \Phi_s) \\ &= \mathbb{P}\left(hR^{-\alpha}/I_{s,s} > T \mid \Phi_s\right) \\ &= \mathbb{E}_{h_i}\left[\mathbb{P}\left(h > TR^\alpha G \cdot \sum_{i=2} h_i l(\theta_i) R_i^{-\alpha} \,\middle|\, \Phi_s\right)\right] \\ &= \prod_{i=2}^{\infty} \frac{G}{1 + Tr^\alpha R_i^{-\alpha}\left(1/e^{|x_i|}\right)}. \end{aligned} \tag{24}$$

From equation (22), M_b can be expressed as

$$M_b = \mathbb{E}_r\left[\mathbb{E}_{r_i}\prod_{i=2}^{\infty}\mathbb{E}_{\theta_i}\left[\left(\frac{G}{1 + Tr^\alpha R_i^{-\alpha}\left(1/e^{|x_i|}\right)}\right)^b\right]\right], \tag{25}$$

where

$$\mathbb{E}_{r_i}\prod_{i=2}^{\infty}\mathbb{E}_{\theta_i}\left[\left(\frac{G}{1 + Tr^\alpha R_i^{-\alpha}\left(1/e^{|x_i|}\right)}\right)^b\right] = \exp\left(-2\lambda_s \times \int_r^\infty \left(\int_0^{\theta/2}\left[1 - \left(\frac{G}{1 + Tr^\alpha v^{-\alpha}(1/e^x)}\right)^b\right]\mathrm{d}x\right) v\ \mathrm{d}v\right). \tag{26}$$

Let $u = T^{-(2/\alpha)} r^{-2} (1/e^x)^{-(2/\alpha)} v^2$, and equation (26) can be simplified as

$$\begin{aligned} &\mathbb{E}_{r_i}\prod_{i=2}^{\infty}\mathbb{E}_{\theta_i}\left[\left(\frac{G}{1 + Tr^\alpha R_i^{-\alpha}\left(1/e^{|x_i|}\right)}\right)^b\right] \\ &= \exp\left(-\lambda_s (TG)^{2/\alpha} r^2 \int_0^{\theta/2} (1/e^x)^{2/\alpha} F\left((TG)^{-(2/\alpha)}(1/e^x)^{-(2/\alpha)}\right)\mathrm{d}x\right). \end{aligned} \tag{27}$$

Let $g = (TG)^{-2/\alpha}(1/e^x)^{-2/\alpha}$, and the function $F_2(g)$ in equation (27) can be expressed as Gaussian hypergeometric function.

Table 1: Simulation parameters.

Parameter	Value
Intensity of BSs, λ_s	$2 * 10^{-5}$
Intensity of BSs, λ_u	$8 * 10^{-4}$
Transmission power of BSs, P_s	30 dBm
Total simulated area, S	1000 m * 1000 m
Effective radiation angle of directional antennas, Ψ	$13\pi/36$, $\pi/2$, $2\pi/3$
Path loss exponent, α	4
Number of subchannels, N_c	40

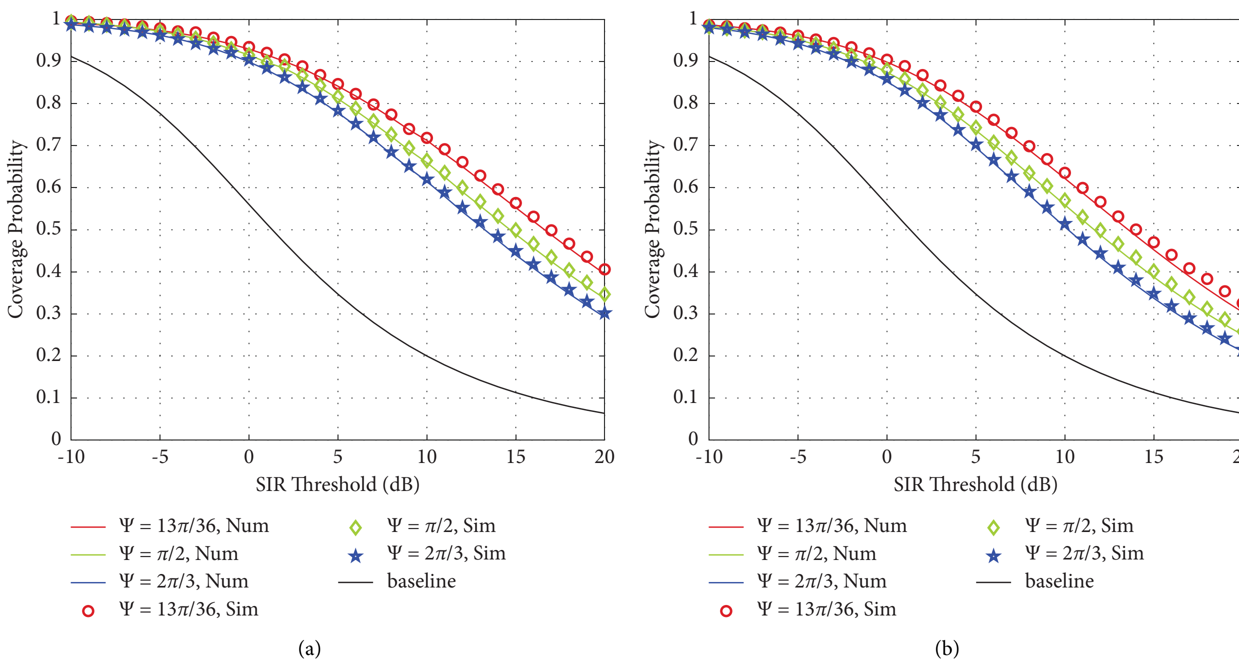

Figure 2: The conditional success probability as a function of SIR threshold under different antenna angles Ψ. (a) Coverage probability of the proposed model with SA-ICIC. (b) Coverage probability of directional model without SA-ICIC.

$$F_2(g) = \int_g^{\infty}\left(1 - \frac{1}{\left(1 + u^{-(\alpha/2)}\right)^b}\right)\mathrm{d}u = g\left(-1 + {}_2F_1\left(-(\alpha/2), b, 1-(\alpha/2), -g^{-(\alpha/2)}\right)\right). \quad (28)$$

From equations (24) and (25), Theorem 3 is obtained. □

Lemma 3. *When $b = -1$, the average local delay before a typical user accesses the network with SA-ICIC strategy is*

$$M_{-1} = \pi\lambda_s \int_0^{\infty} \exp\left(-\lambda_s v C_6(\alpha, T, \Psi) - \lambda_s \pi v\right)\mathrm{d}v, \quad (29)$$

where $C_6(\alpha, T, \Psi) = \int_0^{\Psi/2} 2F_1[-(2/\alpha), -1, 1-(2/\alpha), -Te^{-\theta}G]\mathrm{d}\theta$.

5. Numerical Results

In this section, simulations are performed through MATLAB Monte-Carlo, which validates the numerical result of the SA-ICIC scheme involved in the previous section. The simulation environment is built according to the system model described in Section 2. The following parameters are set according to the LTE-A. Specifically, the network area is 1000m × 1000m, BSs are placed in the establishment area according to PPP with $\lambda_s = 20\text{BSs/km}^2$, and users are randomly placed with $\lambda_u = 800\text{users/km}^2$. The value of path loss exponent α is equal to 4. To improve the readability of the results, reference [12] with non-ICIC was used as the comparison of performance indicators. Ψ is the key parameter of antenna installation. In densely built urban areas, on account of the serious multi-path reflection, the radiation angle of the antenna is generally set at about $13\pi/36$ to reduce the mutual interference of adjacent cells, whereas operators commonly select the antenna angle $13\pi/36$, $\pi/2$ and $2\pi/3$ in the suburbs. Therefore, the antenna angles of $13\pi/36$, $\pi/2$, and $2\pi/3$ are considered in this paper [31]. The reliability of simulation results corresponds to the statistical average of 20000 iterations, so it can more precisely respond to the performance of directional UDNs under the SA-ICIC algorithm. Table 1 summarizes the simulation parameters.

Figure 2 shows the standard success probability of the directional antenna model with the proposed SA-ICIC and

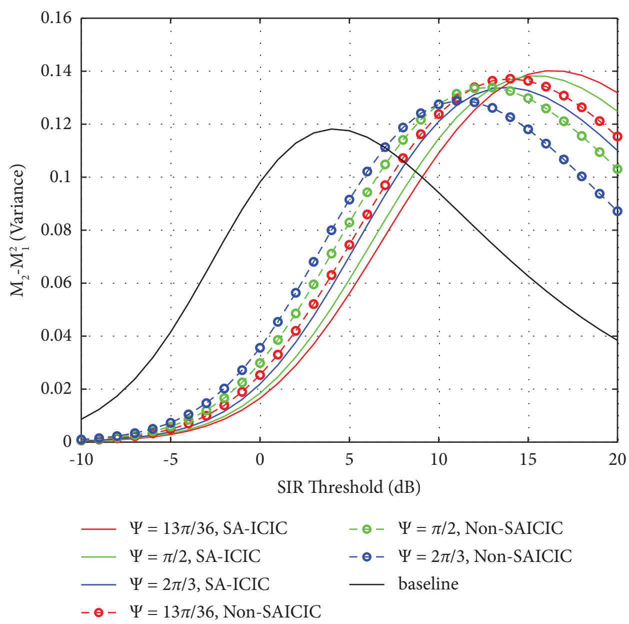

Figure 3: Comparison of variance at different antenna angles Ψ.

that without SA-ICIC. At a given SIR threshold, by comparing Figures 2(a) and 2(b), it can be seen that under different radiation angles Ψ, the coverage probability of the proposed SA-ICIC scheme model is higher than that of the model without our strategy. For example, when $T = 5$dB, the coverage probability with ICIC under radiation angles $\Psi = 13\pi/36$ is 0.84, while the coverage probability with non-SA-ICIC is 0.78. Similarly, the coverage probability with SA-ICIC under radiation angles $\pi/2$ and $2\pi/3$ is 0.82 and 0.78 respectively, while the coverage probability with non-SA-ICIC is 0.75 and 0.71, respectively. This is because users are mainly affected by the interference from the second nearest BS. When users are located within the radiation range of their second nearest BS, the proposed SA-ICIC strategy can reduce or eliminate the interference received from their second nearest BS, so as to improve the coverage probability. Specially, the black baseline is the coverage probability of the isotropic antenna cellular model in reference [32]. This also reflects that the system with SA-ICIC strategy outperforms system without SA-ICIC strategy. In addition, the coverage probability increases with the decrease of the radiation angle Ψ. This means that when Ψ decreases, users are less likely to suffer from severe ICI, which is consistent with the conclusion of reference [12].

Figure 3 shows the variance comparison between the proposed SA-ICIC strategy model of directional antenna and the model without this strategy. As can be seen in Figure 3, the variance with the SA-ICIC strategy is smaller than the variance without this strategy. Thus, the network users with the SA-ICIC strategy can get better and more stable SIR performance. At the same time, the variance of the standard success probability initially increases at low values of SIR threshold T and then decreases at high values of T. The reason is that when the SIR threshold is relatively small, the success probability of users accessing the network is very

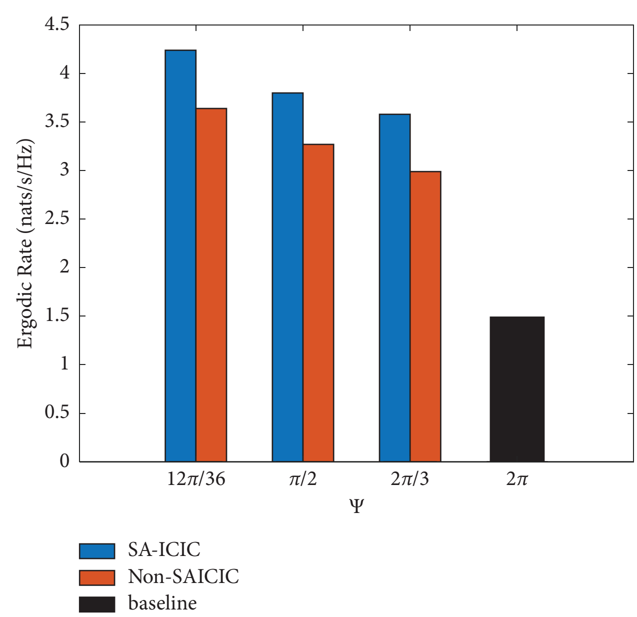

Figure 4: Comparison of average ergodic rates at different antenna angles Ψ.

high whether the proposed ICIC scheme is used or not, while with the increase of SIR threshold, the success probability of users accessing the network decreases, which results in the variance first increasing and then decreasing. Furthermore, when Ψ is relatively small, i.e., $\Psi = 13\pi/36$, if the network adopts the SA-ICIC strategy, the decline phenomenon is not significant. Also, the increasing trend of variance continued when the SA-ICIC strategy was adopted. This proves that with the decrease of Ψ, the communication service quality of all users becomes stable under the proposed ICIC strategy model.

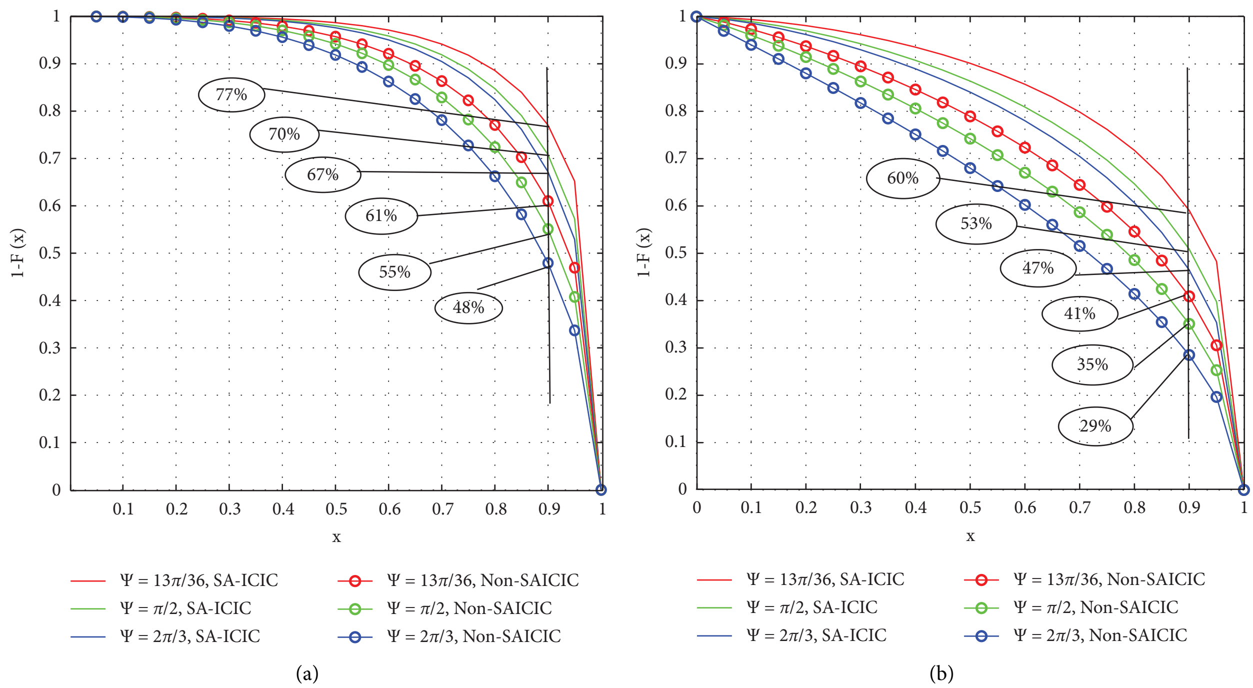

Figure 5: Meta distribution comparison of SIR under different Ψ when T is fixed. (a) $T = 0$ dB. (b) $T = 5$ dB.

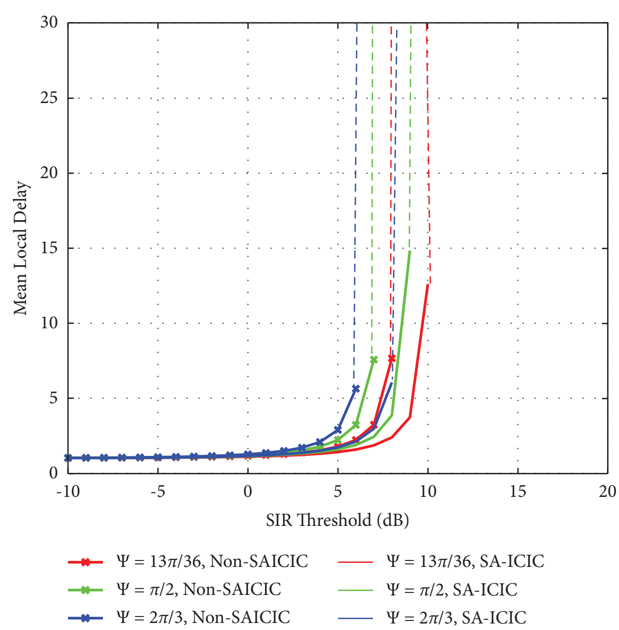

Figure 6: Comparison of mean local delays under different Ψ.

In Figure 4, the average ergodic rates of the two network models are represented by a bar graph. The blue bar and red bar represent the network with the proposed ICIC scheme and the network without the strategy, respectively. As shown in Figure 4, the SA-ICIC scheme provides a higher ergodic rate, which verifies the proposed SA-ICIC scheme can reduce the interference received by the user from its second closest BS. On the other hand, as the antenna angle decreases, the ergodic rate shows an increasing trend. The specific reason for the graph change is consistent with that of the coverage probability described above.

Figure 5 investigates the comparison of the meta distribution of SIR under different conditions x when SIR threshold T remains constant. In Figure 5(a), when $T = 0$ dB, the proportion of users of the network with SA-ICIC whose communication success probability exceeds 0.9 is 77%, 70%, and 67% under different antenna radiation angles $13\pi/36$, $\pi/2$, and $2\pi/3$, respectively, whereas the proportion of users of the network without SA-ICIC whose communication success probability exceeds 0.9 is 61%, 55%, and 48%, respectively. When $T = 5$ dB, there is no doubt that the communication quality of all links will be better than that of $T = 0$ dB in the networks. Consequently, in Figure 5(b), the proportion of users of the network with SA-ICIC whose communication success probability exceeds 0.9 is 60%, 53%, and 47%, respectively, whereas the proportion of users of the network without SA-ICIC whose communication success probability exceeds 0.9 is 41%, 35%, and 29%, respectively. The probability of communication success is significantly higher than that without the SA-ICIC strategy. Therefore, these observations verify that the SA-ICIC strategy can effectively alleviate the interference of UDNs and improve the network performance.

The mean local delay is defined as the mean number of transmissions until the first success [22]. Figure 6 shows the comparison of users' mean local delay with T when the SA-ICIC strategy model of directional antenna is adopted under different Ψ. As shown in Figure 6, the mean local delay curve shifts to the right when Ψ decreases, i.e., when the SIR threshold T is fixed, the mean local delay decreases with Ψ. The UDNs that do not adopt the SA-ICIC strategy have a larger delay because users are subject to greater interference under this scenario. It is worth mentioning that the mean local delay suddenly jumps to infinity when certain SIR thresholds are reached, regardless of whether the SA-ICIC strategy for directional antennas is applied.

6. Conclusions

In this paper, we developed a comprehensive framework for the performance analysis of directional UDNs with a dynamic spectrum allocation strategy, which is suitable for all users because it allows the mitigation of interference from their second nearest BSs. The key idea of our scheme is that when colliding with the beam of other cells, the channel occupied by a user requesting communication will be interlocked with the channel allocated by users within the effective radiation range of the nearest interference BS at the same time through dynamic subchannel allocation. Numerical results show that SA-ICIC provides both coverage and ergodic rate gain. The derived meta distribution of SIR yields significant insights on SA-ICIC strategy from the different service experiences of individual links in the UDNs rather than the generally evaluated average over all users. It is further shown that the UDNs adopting the SA-ICIC scheme effectively reduce the local delay of users.

An extension of this work is to combine resource allocation and multi-antenna BSs to improve the performance of edge users on coverage probability in 3-D cellular networks for the reason that the number of users will be rapidly increased in the future network.

Data Availability

The data supporting this study are from previously reported studies and datasets, which have been cited. The processed data are available from the corresponding author upon request.

Conflicts of Interest

The authors declare that there are no conflicts of interest regarding the publication of this paper.

Acknowledgments

This study was supported by the National Natural Science Foundation of China (NSFC) (61901071) and in part by the General Project of the Natural Science Foundation of Chongqing (cstc2020jcyj-zdxmX0024).

References

[1] J. Bugel, S. John, and S. Schwartz, "Ericsson mobility report," Technical. Report, Ericssion, Kista, Stockholm, Sweden, 2020.

[2] M. A. Adedoyin and O. E. Falowo, "Combination of ultra-dense networks and other 5g enabling technologies: a survey," *IEEE Access*, vol. 8, pp. 22 893–922 932, 2020.

[3] M. Kamel, W. Hamouda, and A. Youssef, "Ultra-dense networks: a survey," *IEEE Communications Surveys & Tutorials*, vol. 18, no. 4, pp. 2522–2545, 2016.

[4] H. O. Kpojime and G. A. Safdar, "Interference mitigation in cognitive-radio-based femtocells," *IEEE Communications Surveys & Tutorials*, vol. 17, no. 3, pp. 1511–1534, 2015.

[5] W. Yang, J. Zhang, and J. Zhang, "On performance of ultra-dense neighborhood small cell networks in urban scenarios," *IEEE Communications Letters*, vol. 25, no. 4, pp. 1378–1382, 2021.

[6] I. T. S. Sesia and M. Baker, *LTE-the UMTS Long Term Evolution: From Theory to Practice*, Wiley, New York, NY, UAS, 2009.

[7] D. Lopez-Perez, I. Guvenc, G. de la Roche, M. Kountouris, T. Q. Quek, and J. Zhang, "Enhanced intercell interference coordination challenges in heterogeneous networks," *IEEE Wireless Communications*, vol. 18, no. 3, pp. 22–30, 2011.

[8] T. Kim, I. Bang, and D. K. Sung, "Design criteria on a mmwave-based small cell with directional antennas," in *Proceedings of the 2014 IEEE 25th Annual International Symposium on Personal, Indoor, and Mobile Radio Communication (PIMRC)*, pp. 103–107, Washington, DC, USA, September 2014.

[9] G. Gougeon, Y. Corre, A. De Domenico et al., "Lte system-level evaluation of directive compact antennas for small-cell networks," in *Proceedings of the 2016 10th European Conference on Antennas and Propagation (EuCAP)*, pp. 1–5, Davos, Switzerland, April 2016.

[10] A.-H. Tsai, "Two-tier interference mitigation with directional antennas for small-cells in an apartment building," in *Proceedings of the 2018 15th International Symposium on Wireless Communication Systems (ISWCS)*, pp. 1–5, Lisbon, Portugal, August 2018.

[11] C. Psomas, M. Mohammadi, I. Krikidis, and H. A. Suraweera, "Impact of directionality on interference mitigation in full-duplex cellular networks," *IEEE Transactions on Wireless Communications*, vol. 16, no. 1, pp. 487–502, 2017.

[12] Q. Liu, J. Zou, and Y. Gu, "Coverage and Meta Distribution Analysis in Ultra-dense Cellular Networks with Directional Antennas," *IEEE Transactions on Vehicular Technology*, vol. 71, pp. 9805–9816, 2022.

[13] M. Li, F. Zhang, Y. Ji, and W. Fan, "Virtual antenna array with directional antennas for millimeter-wave channel characterization," *IEEE Transactions on Antennas and Propagation*, vol. 70, no. 8, pp. 6992–7003, 2022.

[14] T. D. Novlan, R. K. Ganti, A. Ghosh, and J. G. Andrews, "Analytical evaluation of fractional frequency reuse for ofdma cellular networks," *IEEE Transactions on Wireless Communications*, vol. 10, no. 12, pp. 4294–4305, 2011.

[15] A. S. Hamza, S. S. Khalifa, H. S. Hamza, and K. Elsayed, "A survey on inter-cell interference coordination techniques in ofdma-based cellular networks," *IEEE Communications Surveys & Tutorials*, vol. 15, no. 4, pp. 1642–1670, 2013.

[16] Y. Wang, G. Feng, Y. Sun, S. Qin, and Y.-C. Liang, "Decentralized learning based indoor interference mitigation for 5g-and-beyond systems," *IEEE Transactions on Vehicular Technology*, vol. 69, no. 10, pp. 12124–35, 2020.

[17] M. Song, H. Shan, H. H. Yang, and T. Q. S. Quek, "Throughput analysis of small cell networks under d-tdd and ffr," *IEEE Communications Letters*, vol. 25, no. 2, pp. 665–669, 2021.

[18] M. S. Akhtar, Z. H. Abbas, F. Muhammad, and G. Abbas, "Analysis of decoupled association in hetnets using soft frequency reuse scheme," *AEU - International Journal of Electronics and Communications*, vol. 113, Article ID 152961, 2020.

[19] M. S. Haroon, Z. H. Abbas, F. Muhammad, G. Abbas, and F. Y. Li, "Enabling Soft Frequency Reuse and Stienen's Cell Partition in Two-Tier Heterogeneous Networks: Cell Deployment and Coverage Analysis," *IEEE Transactions on Vehicular Technology*, vol. 70, pp. 613–626, 2020.

[20] H. Wei, N. Deng, and M. Haenggi, "Performance analysis of inter-cell interference coordination in mm-wave cellular networks," *IEEE Transactions on Wireless Communications*, vol. 21, no. 2, pp. 726–738, 2022.

[21] H. ElSawy, A. Sultan-Salem, M.-S. Alouini, and M. Z. Win, "Modeling and analysis of cellular networks using stochastic geometry: a tutorial," *IEEE Communications Surveys & Tutorials*, vol. 19, no. 1, pp. 167–203, 2017.

[22] M. Haenggi, "The meta distribution of the sir in Poisson bipolar and cellular networks," *IEEE Transactions on Wireless Communications*, vol. 15, no. 4, pp. 2577–2589, 2016.

[23] A. Ullah, Z. Haq Abbas, G. Abbas, F. Muhammad, and L. Jiao, "Performance analysis of user-centric sbs deployment with load balancing in heterogeneous cellular networks: a thomas cluster process approach," *Computer Networks*, vol. 170, Article ID 107120, 2020.

[24] X. Zhang and M. Haenggi, "A stochastic geometry analysis of inter-cell interference coordination and intra-cell diversity," *IEEE Transactions on Wireless Communications*, vol. 13, no. 12, pp. 6655–6669, 2014.

[25] J. Yoon and G. Hwang, "Distance-based inter-cell interference coordination in small cell networks: stochastic geometry modeling and analysis," *IEEE Transactions on Wireless Communications*, vol. 17, no. 6, pp. 4089–4103, 2018.

[26] W. K. New, C. Y. Leow, K. Navaie, Y. Sun, and Z. Ding, "Interference-aware noma for cellular-connected uavs: stochastic geometry analysis," *IEEE Journal on Selected Areas in Communications*, vol. 39, no. 10, pp. 3067–3080, 2021.

[27] J. G. Andrews, A. K. Gupta, and H. S. Dhillon, "A Primer on Cellular Network Analysis Using Stochastic Geometry," 2016, https://arxiv.org/abs/1604.03183.

[28] T. Zhang, J. Zhao, L. An, and D. Liu, "Energy efficiency of base station deployment in ultra dense hetnets: a stochastic geometry analysis," *IEEE Wireless Commun. Lett.*vol. 5, no. 2, pp. 184–187, 2016.

[29] Q. Liu, Z. Zhang, H. Hu, and J. Shi, "Modeling and analysis of one-tier ultradense multiuser networks," *IEEE Access*, vol. 6, pp. 13972–13979, 2018.

[30] L. Yang, F.-C. Zheng, Y. Zhong, and S. Jin, "Spatio-temporal analysis of meta distribution for cell-center/cell-edge users," *IEEE Transactions on Communications*, vol. 69, no. 12, pp. 8256–8270, 2021.

[31] D. B. Miron and F. I. Antenna, *Small Antenna Design*, Elsevier, Amsterdam, Netherlands, 2006.

[32] J. G. Andrews, F. Baccelli, and R. K. Ganti, "A tractable approach to coverage and rate in cellular networks," *IEEE Transactions on Communications*, vol. 59, no. 11, pp. 3122–3134, 2011.